Quantum Mechanical Studies of CH₃ClO₃ Isomers and the CH₃O₂+ClO Reaction Pathways

Evangelos Drougas,[†] **Abraham F. Jalbout,**[‡,§] **and Agnie M. Kosmas*,**[†]

Department of Chemistry, University of Ioannina, Greece 451 10, Department of Physics, Dillard University, New Orleans, Louisiana 70112, and Department of Chemistry, The University of New Orleans, New Orleans, Louisiana 70148

The geometries, harmonic vibrational frequencies, and relative energetics of CH_3ClO_3 isomers have been examined using quantum mechanical methods. At the G2MP2 level of theory, the lowest-energy structure is found to be the CH_3OClO_2 form followed by the chain-type CH_3OOOCl isomer located 7.9 kcal mol^{-1} higher. The QCISD(T) method predicts that the CH_3OOOCl structure is located lower than CH_3OClO_2. The two higher-energy structures are CH_3OOClO and CH_3ClO_3 across all energy levels. Interisomerization transition states have been determined, and the role of the formation of CH_3ClO_3 structures in the various pathways of the reaction $CH_3O_2 + ClO$ is also examined.

1. Introduction

The reaction between methylperoxy radicals and chlorine monoxide

$$ClO + CH_3O_2 \rightarrow products \qquad (1)$$

has been strongly suggested to play an interesting role in the CH_4 oxidation chain, and thus, to contribute to yet another possible ozone-depletion cycle in the chemistry of the polar atmosphere.[1] Hence, several experimental studies[2−9] have been carried out for this system.

The first measurement[2] of the rate constant for reaction 1 was made using the molecular-modulation technique, generating both CH_3O_2 and ClO in the broad band photolysis of a $Cl_2−CH_4−Cl_2O−O_2$ mixture at 300 K and at a pressure of 230−240 Torr. A rate constant of $(3.1 \pm 1.7) \times 10^{-12}$ cm^3 molecule^{-1} s^{-1} was derived, and the product analysis studies enabled the authors to conclude that the major reaction channel (85 ± 15)% leads to $CH_3O + ClOO$ formation, i.e., to O_2 and active chlorine

$$CH_3O_2 + ClO \rightarrow CH_3O + ClOO \rightarrow CH_3O + Cl + O_2 \quad (1a)$$

Other species such as CH_3OCl, OClO, and O_3 were not detected, and consequently the possibility of other reaction pathways has been considered to be negligible. DeMore[3] undertook a low-temperature study (197−217 K) of reaction 1 by employing photolysis of $Cl_2−CH_4−O_3−O_2−N_2$ mixtures to generate ClO and CH_3O_2. In his study, an upper limit of 4×10^{-12} cm^3 molecule^{-1} s^{-1} at 200 K was adopted for channel 1a with the assumption of negligible contributions from any other channels. On the basis of the importance of channel 1a, Crutzen et al.[1] have reported an interesting modeling study showing that reaction 1a coupled with the heterogeneous reaction HCl + HOCl → Cl_2 + H_2O may explain the accelerated rates of ozone depletion caused by active chlorine. However, more detailed kinetic and product-branching data were reported later in the

work of Helleis et al.[4] in the temperature range 225−355 K and constant pressure conditions, using the discharge-flow/mass spectrometry technique. In their work, CH_3OCl was detected in the products and thus, channel 1b was identified

$$CH_3O_2 + ClO \rightarrow CH_3OCl + O_2 \qquad (1b)$$

They reported roughly equal rate constants of 1×10^{-12} cm^3 molecule^{-1} s^{-1} for each channel at the low-temperature region prevalent in the polar winter and the early springtime stratosphere and a decreasing branching ratio for 1a as the temperature decreases. They thus established CH_3OCl as a potentially important species in ozone-hole chemistry. Several other studies[5−9] followed, leading to similar conclusions about the significance of both these channels. Nevertheless, large discrepancies were obtained with respect to the branching ratio values, k_{1a}/k, at 298 K, and the various results as summarized by Daele and Poulet[9] are very scattered, ranging from 0.3 to 0.9.

In the present work, we examine the possibility of the formation of CH_3ClO_3 complexes from the $CH_3O_2 + ClO$ reaction. Quantum mechanical techniques have been employed to examine the structural characteristics and the relative energetics of the CH_3ClO_3 isomers and the saddle point configurations leading to various possible production pathways. Finally, a comparison is carried out with the H- and Br-analogous systems, ClO + HO_2,[10−14] BrO + HO_2,[15,16] and CH_3O_2 + BrO.[17,18]

2. Quantum Mechanical Calculations and Results

The geometries of all reactants, products, and stationary points have been fully optimized at the UMP2(full)/6-31G(d) level of theory. Harmonic frequencies have also been calculated at the same level to characterize the stationary points, and internal reaction coordinate calculations were performed to confirm that each transition state is indeed linked to the appropriate reactants and products. Transition-state structures were identified by one imaginary frequency as first-order saddle points. Next, G2MP2[19] calculations were carried out at the UMP2(full)/6-31G(d)-optimized geometries in order to refine the energetics. The G2MP2 method is a modified version of G2[20] using MP2 instead

* Author to whom correspondence may be addressed. E-mail: amylona@cc.uoi.gr.
† University of Ioannina.
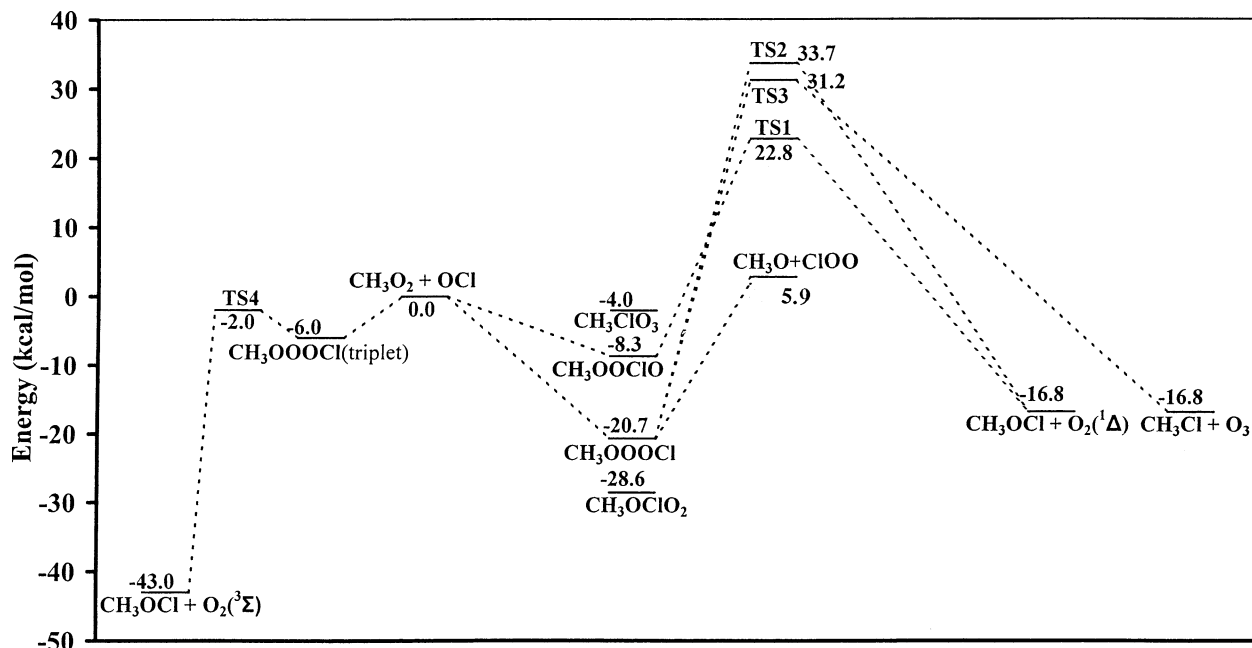‡ Dillard University.
§ The University of New Orleans.

Quantum Mechanical Studies of CH₃ClO₃ Isomers

J. Phys. Chem. A, Vol. 107, No. 51, 2003 **11387**

Figure 1. Energy profile at the G2MP2 level for the reaction $CH_3O_2 + ClO$, main channels being $CH_3O + ClOO$ and $CH_3OCl + O_2$.

of MP4 for the basis set extension corrections. All calculations were performed using the Gaussian 98 series of programs.[21]

Five isomeric minimum-energy structures, three isomerization transition-state geometries, and four transition-state configurations leading to various production pathways were determined in total. The $CH_3OCl + O_2$ pathway has been studied on both the singlet and triplet surfaces. The overall energy profile based on the G2MP2 results is depicted in Figure 1, while the optimized structures for the intermediate minima and the transition-state configurations at the UMP2(full)/6-31G(d) level of theory are depicted in Figure 2. The calculated electronic energies at the G2MP2 level of theory and the corresponding relative energetics are collected in Table 1. The relative energetics for the two lowest-energy structures were also investigated at the G3 theory level and are included in Table 2.

Further investigation of the four isomeric energy minima on the singlet surface has been carried out using the quadratic configuration interaction with single and double excitations (QCISD) method. Optimized geometries have been obtained in conjunction with the 6-31G(d) basis set, which agree within less than 5% with the MP2/ 6-31G(d)-optimized structures. To improve the energies, single-point calculations were further performed using the QCISD(T) method in combination with the higher basis sets (d,p), (2d,2p), and (2df,2p). Table 2 contains the QCISD(T) electronic energies of the four isomeric structures in conjuction with the various basis sets employed.

3. CH₃ClO₃ Isomers

3.1. Structures and Frequencies of CH₃ClO₃ Isomers. Four isomeric local-minimum energy structures were located on the singlet surface and one on the triplet. The first isomeric minimum investigated is the straight chain type structure CH_3-$OOOCl$ in the singlet state, which is found to possess a skewed geometry and resemble closely the CH_3OOOBr minimum-energy structure.[16,17] The detailed geometrical parameters are given in Figure 2. Of interest is the overall similarity with the stratospherically important HOOOCl species.[10,11,13,14] For instance, the CO−OO and OO−OCl bond lengths in CH_3OOOCl, 1.436 and 1. 433 Å, respectively, at the present MP2/ 6−31(d) level compare well with the corresponding HO−OO and OO−
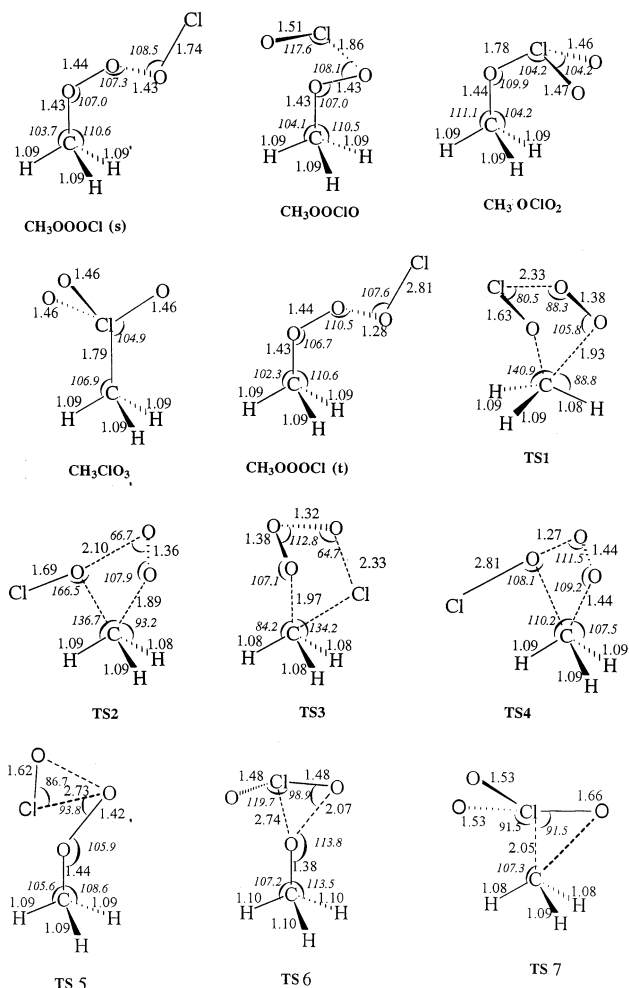

Figure 2. Structures for stationary points on the potential-energy surface of reaction $CH_3O_2 + ClO$.

OCl bond lengths in HOOOCl, 1.434 and 1.429 Å, at the same theory level.[11] We have the same type of bonding in CH_3OOOCl and HOOOCl as in the case of Br-containing species, CH_3-$OOOBr$ and HOOOBr, discussed by Guha and Francisco.[16]

TABLE 1: Total Electronic (Hartrees) and Relative Energies (kcal mol^{-1}) for Various Species Involved in CH$_3$O$_2$ + ClO Reaction Pathways

species	MP2/6-31G(d)	ΔE	G2MP2	ΔE	ZPE
CH$_3$O$_2$ + ClO	−724.127637	0.0	−724.678756	0.0	29.4
CH$_3$OOOCl (s)	−724.164944	−21.8	−724.711724	−20.7	30.9
CH$_3$OOClO	−724.148882	−12.0	−724.691944	−8.3	30.7
CH$_3$OClO$_2$	−724.157233	−16.1	−724.724392	−28.6	31.9
CH$_3$ClO$_3$	−724.095129	24.1	−724.685179	−4.0	33.1
CH$_3$OOOCl (t)	−724.140453	−5.6	−724.688315	−6.0	31.8
TS1	−724.095649	20.4	−724.642431	22.8	29.7
TS2	−724.087899	24.9	−724.625132	33.6	29.4
TS3	−724.088323	27.2	−724.628981	31.2	31.9
TS4	−724.136235	−3.3	−724.681873	−2.0	31.4
TS5	−724.101457	16.2	−724.651232	17.3	29.1
TS6	−724.111307	5.8	−724.685989	−4.5	24.9
TS7	−724.019056	66.7	−724.565675	91.6	28.0
CH$_3$O+ClOO	−724.108866	11.3	−724.669321	5.9	28.8
CH$_3$OCl + O$_2$($^1\Delta$)	−724.186654	−34.6	−724.705501	−16.8	31.8
CH$_3$OCl + O$_2$($^3\Sigma$)	−724.236051	−68.3	−724.747252	−43.0	29.1
CH$_3$Cl + O$_3$	−724.189502	−35.6	−724.705538	−16.8	32.6

The second isomeric form considered is CH$_3$OOClO. This is also a chain-type skewed structure with oxygen as the terminal atom. As in the corresponding CH$_3$OOBrO case, the lone pairs of electrons on the terminal oxygen atom tend to enter into resonance with the Cl—O bond pair, due to which the Cl—O bond attains a partial double-bond character. Such a resonance effect is not observed with the oxygen atoms that are sandwiched between the carbon and the chlorine atoms. The fact is also manifested by inspecting the dihedral angles between COOCl and OOClO atoms, 93.3 and 86.9°respectively. The geometry indicates right angles between the CO—ClO and OO—ClO bonds, consistent with the partial double-bond character for OOCl=O. As a result, the Cl—O bond, 1.510 Å, is much shorter than the O—Cl bond, 1.859 Å, comparing very well with the corresponding values in HOOClO, 1.511 and 1.874 Å, at the same MP2/6-31G(d) level. Thus, CH$_3$OOClO also presents similar bonding characteristics as HOOClO.

The other two forms are CH$_3$OClO$_2$ and CH$_3$ClO$_3$. The effect of the partial double-bond character between chlorine and the terminal oxygen atoms is enhanced. Again, this is due to the lone pairs of electrons on the terminal oxygen atoms that enter into partial resonance with their immediate bonding electron neighbors, thus, rendering double-bond character to the terminal Cl—O bonds. Consequently, the Cl—O bond distances in CH$_3$-OClO$_2$ are even shorter, 1.466 Å, than the OCl distance of 1.776 Å (1.466 and 1.754 Å in HOClO$_2$, respectively, at the same level of theory).[11] The resonance effect is more prominent in the fourth isomeric form, CH$_3$ClO$_3$, with the three oxygen atoms forming the base of a pyramid. In this case, resonance plays an even stronger role than in CH$_3$OOClO and CH$_3$OClO$_2$, making the Cl=O double-bond character quite pronounced. As a result, the ClO bond distance in CH$_3$ClO$_3$, 1.458 Å, is the shortest among all isomers.

Finally, a loose, chain-type CH$_3$OOOCl structure was determined on the triplet surface. The triplet surface was examined due to the need of investigating the CH$_3$OCl + O$_2$($^3\Sigma$) reaction pathway. Its geometry is found to be close to that of CH$_3$-OOOCl(s), with differences encountered only for the OO—OCl and O—Cl equilibrium distances (1.276, 2.807 Å) compared to the corresponding values in the singlet state (1.433, 1.741 Å). In particular, we note the increase in the O—Cl bond distance exceeding 1 Å as a result of the triplet electronic configuration of the adduct.

The calculated vibrational frequencies are collected in Table 3 of Supporting Information. Their classification follows the same description as those of (CH$_3$BrO$_3$) species.[16−17]

3.2. Relative Energetics of CH$_3$ClO$_3$ Isomers. The calculated energies for the minimum-energy isomers of CH$_3$ClO$_3$ are summarized in Table 1. At the MP2(full)/6−31(d) level of theory, the order of relative stability among the isomers on the singlet surface (from the most stable to the least stable structure) is CH$_3$OOOCl > CH$_3$OClO$_2$ > CH$_3$OOClO > CH$_3$ClO$_3$ in full analogy with the HClO$_3$ family at the same level of theory.[11] However, when employing the G2MP2 theory, this order is partially inversed and becomes CH$_3$OClO$_2$ > CH$_3$OOOCl > CH$_3$OOClO > CH$_3$ClO$_3$. This inversion is quite analogous with what has been observed by Guha and Francisco in the HClO$_3$,[11] HBrO$_3$,[15] and CH$_3$BrO$_3$[17] families. As they have discussed in detail, the relative stability ordering among these species is very sensitive both to basis set size and the methodology used. Use of G1 and G2 theories has caused the partial inversion of their B3LYP and MP2 predicted stabilities and placed the HOClO$_2$, HOBrO$_2$, and CH$_3$OBrO$_2$ forms lower in energy than the corresponding isomers with all oxygen atoms in the middle. An analogous inversion is observed here too. CH$_3$OClO$_2$ is found to be the most stable structure at the G2MP2 level followed by CH$_3$OOOCl, located higher by 7.9 kcal mol^{-1}. The CH$_3$OOClO and CH$_3$ClO$_3$ structures remain higher in energy, located at 12.4 and 16.7 kcal mol^{-1}, respectively, with respect to CH$_3$OOOCl at the G2MP2 level.

Recently, Guha and Francisco[18] have re-examined the stability ordering of CH$_3$BrO$_3$ isomers, using the quadratic configuration interaction method in combination with various basis sets of increasing order. They have found the following stability ordering CH$_3$OOOBr > CH$_3$OBrO$_2$ > CH$_3$OOBrO > CH$_3$BrO$_3$. Namely, they have found that the CH$_3$OOOBr isomer is the lowest-energy structure and that CH$_3$OBrO$_2$ is higher in energy by 1.4 kcal mol^{-1} at the QCISD(T)/6-311G(2df,2p) level of theory. To compare the stability trends in the CH$_3$ClO$_3$ family with those of CH$_3$BrO$_3$, we have also employed the quadratic configuration interaction method in combination with various basis sets of increasing level to calculate the relative energetics of the minimum-energy structures. Optimization has been carried out at the QCISD/6-31G(d) level, as already mentioned, producing similar geometries with the MP2(full)/6-31G(d) method, with differences never exceeding 5%. The resulting energetics are summarized in Table 2. It is quite interesting to realize that the same inversion takes place in the CH$_3$ClO$_3$ family as well. Thus, the CH$_3$OOOCl isomer is also calculated to be the lowest-energy structure, and the CH$_3$OClO$_2$ form is found to lie higher in energy by 4.2 kcal mol^{-1} (including ZPE corrections) at the QCISD(T)/6-311G(2df,2p) level of theory. The other two isomers have been found to lie higher in energy across all levels of theory. Table 2 also contains the G3 results for these two isomers. We can see that the G3 methodology produces the same trends as G2MP2.

In our opinion, the high stability of the CH$_3$OClO$_2$ form, which competes with that of the chain-type CH$_3$OOOCl, is a consequence of the enhanced stabilization acquired by XClO$_2$ and XBrO$_2$ species in general, as the electronegative character of the X fragment increases. The subject has been extensively studied by Lee et al.,[24] and it has been clearly shown for a number of XClO$_2$ and XBrO$_2$ adducts.[25,26] The halogen atom, Cl or Br, due to its hypervalent character in this type of compound, is found to be very positively charged, so that bonding to an electronegative partner such as HO− or CH$_3$O− greatly enhances the stability of these species.

4. Reaction Pathways and Isomerization

4.1. Transition-State Configurations. From the potential-energy minima discussed earlier, only CH$_3$OOOCl and CH$_3$-

Quantum Mechanical Studies of CH$_3$ClO$_3$ Isomers

J. Phys. Chem. A, Vol. 107, No. 51, 2003 **11389**

TABLE 2: Energetics of the Four Isomeric Structures (Including ZPE Corrections)^a

theory	CH$_3$OOOCl (s)		CH$_3$OClO$_2$(s)		CH$_3$OOClO(s)		CH$_3$ClO$_3$(s)	
MP2/6-31G(d)	−724.164944	0.0	−724.157233	5.8	−724.148882	10.1	−724.095129	46.0
G2MP2	−724.711724	0.0	−724.724392	−7.9	−724.691944	12.4	−724.685179	16.7
G3	−725.235548	0.0	−725.248752	−8.3				
QCISD(T)/6-311G(d,p)	−724.454003	0.0	−724.401185	34.1	−724.396526	36.1	−724.335629	76.3
QCISD(T)/6-311G(2d,2p)	−724.549621	0.0	−724.527403	14.9	−724.506619	27.0	−724.459624	58.6
QCISD(T)/6-311G(2df,2p)	−724.666925	0.0	−724.661866	4.2	−724.635921	19.4	−724.594915	47.2

^{a} The first column under each species gives the total electronic energy in Hartrees while the second column gives the energy difference of each species in kcal mol^{-1}, with respect to the CH$_3$OOOCl(s) isomer, including ZPE corrections.

OOClO can be formed as nascent products of the CH$_3$O$_2$ + ClO reaction. The main reaction channels on the singlet CH$_3$O$_2$ + ClO surface, considered in the present work are

$$CH_3O_2 + ClO \rightarrow CH_3O + ClOO \qquad (1a)$$

$$\rightarrow CH_3OCl + O_2(^1\Delta)(s) \qquad (1b)$$
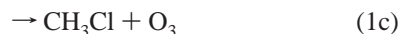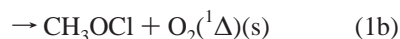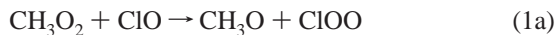
$$\rightarrow CH_3Cl + O_3 \qquad (1c)$$

We have located three transition-state configurations corresponding to the decomposition pathways of the two association adducts and specifically to the pathways: CH$_3$OOClO → CH$_3$-OCl + O$_2$($^1\Delta$), CH$_3$OOOCl(s) → CH$_3$OCl + O$_2$($^1\Delta$), and CH$_3$-OOOCl(s) → CH$_3$Cl + O$_3$, denoted hereafter as TS1, TS2, and TS3, respectively. They each present one imaginary frequency, and they are characterized as first-order saddle points. The structures for the transition states, including the geometrical parameters, are given in Figure 2.

The transition state TS1, encountered in the CH$_3$O$_2$ + ClO → CH$_3$OCl + O$_2$($^1\Delta$) pathway through the CH$_3$OOClO intermediate, is a nonplanar, five-center structure located 22.4 kcal mol^{-1} above reactants and 31.1 kcal mol^{-1} with respect to CH$_3$-OOClO. By comparison of the O−Cl bond distance in TS1 and the CH$_3$OOClO minimum, we find that it is significantly elongated from 1.859 to 2.327 Å in TS1 and the O−O bond length is shortened from 1.431 to 1.378 Å. Also, the C−O bond length increases from 1.431 to 1.926 Å. Yield of the same products, CH$_3$OCl + O$_2$($^1\Delta$), is possible through the formation of the CH$_3$OOOCl(s) minimum, which also involves a nonplanar, four-center transition state, denoted TS2, depicted in Figure 2. TS2 is located higher than TS1 at 33.7 kcal mol^{-1} above reactants. The COOO dihedral angle of −52.7° is considerably different from the dihedral angle, 77.9° in the CH$_3$OOOCl(s) minimum, and the CO−OO bond length, 1.363 Å, is significantly shorter than the corresponding bond distance in the minimum, 1.436 Å. The OO−OCl distance becomes 2.099 Å in TS2 from 1.433 Å in CH$_3$OOOCl(s) and the C−O bond distance 1.886 Å from 1.434 Å. The other pathway by which the CH$_3$OOOCl(s) intermediate may decompose is toward the CH$_3$Cl + O$_3$ products. This pathway also involves a five-center, nonplanar transition state TS3, with C−O and O−Cl bonds considerably elongated, 1.926 and 2.327 Å, relative to 1.434 and 1.741 Å, respectively, in the CH$_3$OOOCl(s) intermediate. TS3 is located 31.2 kcal mol^{-1} above reactants.

Apart from the three reaction pathways through TS1, TS2, and TS3 described above, there is also the possibility of the barrierless CO−OO bond fission process, CH$_3$OOOCl(s) → CH$_3$O + ClOO. The products, the methoxy radical and ClOO, which readily decomposes releasing atomic chlorine, are found to be located at an energy of 5.9 kcal mol^{-1} above reactants at the G2MP2 level, representing the critical energy for this reaction channel. No transition state has been determined for this bond scission channel which thus leads directly to products and reproduces stratospherically active chlorine without an

intervening energy barrier. Thus, from the analysis of all reaction channels discussed so far, this route appears to be thermodynamically the most favorable and it is indeed the channel which has been extensively investigated experimentally. A similar O−O bond fission process of CH$_3$OOClO might be thought to be possible, leading to CH$_3$O + OClO products. However, CH$_3$-OOClO lies higher than CH$_3$OOOOCl(s), and OClO is also known to lie higher than ClOO,[22,23] making such a route less favorable.

Finally, the triplet surface has been investigated in order to examine the

$$CH_3O_2 + ClO \rightarrow CH_3OCl + O_2(^3\Sigma)(t) \qquad (1b)$$

reaction pathway. The triplet surface was found to be much simpler as in the case of the similar HO$_2$ + ClO system.[10,12,13] The loosely bound minimum CH$_3$OOOCl(t), is found, already discussed, and a transition state, TS4, was located for which the analysis of the vibrational frequencies indicated that the structure is a first-order saddle point. Thus, the reaction on the triplet surface occurs through the intermediate formation of the shallow CH$_3$OOOCl(t) minimum bound only by 6 kcal mol^{-1} with respect to reactants. The system further proceeds into the products CH$_3$OCl + O$_2$($^3\Sigma$) through a weak barrier corresponding to TS4 and located at 4 kcal mol^{-1} above CH$_3$OOOCl(t) at the G2MP2 level. As we can see, the energy differences associated with the triplet surface are much smaller as in the case of the HO$_2$ + ClO → HOCl + O$_2$($^3\Sigma$) reaction.[10,13] We can thus conclude that this route provides a thermodynamically feasible reaction pathway towards the formation of CH$_3$OCl + O$_2$($^3\Sigma$) products.

4.2. Isomerization Transition-State Configurations. Three isomerization transition-state configurations have been determined for the isomerization processes, CH$_3$OOOCl ↔ CH$_3$-OOClO, CH$_3$OOClO ↔ CH$_3$OClO$_2$, and CH$_3$OClO$_2$ ↔ CH$_3$-ClO$_3$, denoted hereafter as TS5, TS6, and TS7, respectively. The structures possess one imaginary frequency each, and they are characterized as first-order saddle points. The geometries are provided in Figure 2.

The CH$_3$OOOCl ↔ CH$_3$OOClO isomerization transition state, TS5, is formed due to the migration of the chlorine atom in CH$_3$OOOCl(s). The associated structural changes involve the shrinkage of the O−Cl distance from 1.741 to 1.621 Å and of the CO−OO bond from 1.436 to 1.427 Å in the transition state, respectively. The associated energy barrier is quite high, located at 38.0 kcal mol^{-1} above CH$_3$OOOCl(s) at the G2MP2 level and 17.3 kcal mol^{-1} above the reactants. TS6 represents the transition state for the CH$_3$OOClO ↔ CH$_3$OClO$_2$ isomerization. It is also the result of chlorine migration which produces various structural changes compared to stable CH$_3$OOClO structure. Thus, the O−Cl and Cl−O distances in CH$_3$OOClO, 1.859 and 1.510 Å, approach and become 1.482 and 1.479 Å respectively.

Significant decrease is obtained in the C−O bond distance from1.431 Å in the stable species to 1.377 Å in TS6. The CO−OO is considerably elongated to 2.068 Å, eventually leading to the breaking of the bond while Cl approaches the O bonded to the carbon atom. The bond angles also suffer various changes with the most significant the decrease of the OOCl angle from 108° in the stable species to 99° in TS6 and the increase of the COO bond angle from 107° to 114°, respectively. This transition-state configuration is located lower, at 3.8 kcal mol^{-1} above CH_3OOClO at the G2MP2 level. The three-center geometry of TS6 presents a good analogy with the corresponding transition state structure for HOOClO ↔ HOClO$_2$ isomerization, which is also relatively low, located at the G2M level.[14]

The final isomerization transition state investigated describes the CH_3OClO_2 ↔ CH_3ClO_3 proces due to the migration of the Cl atom in CH_3OClO_2. The O−Cl bond distance of 1.776 Å in CH_3OClO_2 decreases to 1.662 Å to eventually give the third hypervalent Cl−O bond in CH_3ClO_3, while the C−O bond increases to 2.315 Å. It is very high located in consistency with the all analogous energy barriers encountered in the similar isomerization processes of $HClO_3$, $HBrO_3$, and CH_3BrO_3 systems.

5. Summary

Quantum mechanical calculations have been performed to characterize all isomeric forms of the CH_3ClO_3 system. The geometrical parameters and harmonic frequency calculations at the MP2/6−31(d) level of theory show analogous trends with the $HClO_3$, $HBrO_3$, and CH_3BrO_3 families. The energy ordering calculated at the G2MP2 level of theory is CH_3OClO_2 < CH_3-$OOOCl$ < CH_3OOClO < CH_3ClO_3. G3 calculations for the two lowest-energy structures reconfirm the G2MP2 results.

The calculations show that the formation of CH_3OOClO and CH_3OOOCl intermediates on the singlet surface in the course of the CH_3O_2 + ClO reaction is energetically favorable, but further progression into products involves high energy barriers. The barrierless bond fission of CH_3OOOCl(s) into CH_3O + ClOO is found to be the most thermodynamically feasible channel on the singlet surface. The reactive pathway to CH_3-OCl + O_2($^3\Sigma$) on the triplet surface is also found to be thermodynamically favorable. Therefore, the results of the calculations are in good consistency with the experimental findings, which have established these two processes leading to CH_3O + ClOO (1a) and CH_3OCl + O_2(1b) as the two most important reaction pathways.

Regarding the relative stability order of the isomeric forms of the CH_3ClO_3 system, further investigation of the four isomeric structures employing the QCISD(T) methodology with large basis sets partially inverse the G2MP2 results. They produce the chain-type structure CH_3OOOCl(s) as the most stable one as it has been similarly observed in the (CH_3BrO_3) case.[17]

Supporting Information Available: Supporting Information includes two tables that present the structural parameters for the intermediate minima and the transition states, respectively, and a third table that summarizes the harmonic vibrational frequencies of all stationary points. This material is available free of charge via the Internet at http://pubs.acs.org.

References and Notes

(1) Crutzen, P. J.; Muller, R.; Bruhl, C.; Peter, T. *Geophys. Res. Lett.* **1992**, *19*, 1113.

(2) Simon, F. G.; Burrows, J. P.; Schneider, W.; Moortgat, G. K.; Crutzen, P. J. *J. Phys. Chem.* **1989**, *93*, 7807.

(3) DeMore, W. B. *J. Geophys. Res.* **1991**, *96*, 4995.

(4) Helleis, F.; Crowley, J. N.; Moortgat, G. K. *J. Phys. Chem.* **1993**, *97*, 11464.

(5) Kenner, R. D.; Ryan, K. R.; Plumb, J. C. *Geophys. Res. Lett.* **1993**, *20*, 1571.

(6) Kukui, A. S.; Jungkamp, T. P. W.; Schindler, R. N. *Ber. Bunsen−Ges.* **1994**, *98*, 1298.

(7) Helleis, F.; Crowley, J. N.; Moortgat, G. K. *Geophys. Res. Lett.* **1994**, *21*, 1795.

(8) Biggs, P.; Canosa-Mas, C. E.; Frachebound, J. M.; Shallcross, D. E.; Wayne, R. P. *Geophys. Res. Lett.* **1995**, *22*, 1221.

(9) Daele, V.; Poulet, G. *J. Chim. Phys.* **1996**, *93*, 1081.

(10) Buttar, D.; Hirst, D. M. *J. Chem. Soc., Faraday Trans.* **1994**, *90*, 1811.

(11) Francisco, J. S.; Sander, S. P. *J. Phys. Chem.* **1996**, *100*, 573.

(12) Nickolaisen, S.; Roehl, C. M.; Blakeley, L. K.; Friedl, R. R.; Francisco, J. S.; Liu, R.; Sander, S. P. *J. Phys. Chem. A* **2000**, *104*, 308.

(13) Kaltsoyannis, N.; Rowley, D. M. *Phys. Chem. Chem. Phys.* **2000**, *4*, 419.

(14) Xu, Z−F.; Zhu, R.; Lin, M. C. *J. Phys. Chem. A* **2003**, *107*, 1040.

(15) Guha, S.; Francisco, J. S. *J. Phys. Chem. A* **1998**, *102*, 2072.

(16) Guha, S.; Francisco, J. S. *J. Phys. Chem. A* **1999**, *103*, 8000.

(17) Guha, S.; Francisco, J. S. *J. Phys. Chem. A* **2000**, *104*, 3239.

(18) Guha, S.; Francisco, J. S. *J. Chem. Phys.* **2003**, *118*, 1779.

(19) Curtiss, L. A.; Raghavachari, K.; Pople, J. A. *J. Chem. Phys.* **1993**, *98*, 1293.

(20) Curtiss, L. A.; Raghavachari, K.; Trucks, G. W.; Pople, J. A. *J. Chem. Phys.* **1991**, *94*, 7221.

(21) Frisch, M. J.; Trucks, G. W.; Schlegel, H. B.; Scuseria, G. E.; Robb, M. A.; Cheeseman, J. R.; Zakrzewski, V. G.; Montgomery, J. A., Jr.; Stratmann, R. E.; Burant, J. C.; Dapprich, S.; Millam, J. M.; Daniels, A. D.; Kudin, K. N.; Strain, M. C.; Farkas, O.; Tomasi, J.; Barone, V.; Cossi, M.; Cammi, R.; Mennucci, B.; Pomelli, C.; Adamo, C.; Clifford, S.; Ochterski, J.; Petersson, G. A.; Ayala, P. Y.; Cui, Q.; Morokuma, K.; Malick, D. K.; Rabuck, A. D.; Raghavachari, K.; Foresman, J. B.; Cioslowski, J.; Ortiz, J. V.; Stefanov, B. B.; Liu, G.; Liashenko, A.; Piskorz, P.; Komaromi, I.; Gomperts, R.; Martin, R. L.; Fox, D. J.; Keith, T.; Al-Laham, M. A.; Peng, C. Y.; Nanayakkara, A.; Gonzalez, C.; Challacombe, M.; Gill, P. M. W.; Johnson, B. G.; Chen, W.; Wong, M. W.; Andres, J. L.; Head-Gordon, M.; Replogle, E. S.; Pople, J. A. *Gaussian 98*, Gaussian, Inc.: Pittsburgh, PA, 1998.

(22) Pacios, L. F.; Gomez, P. C. *J. Phys. Chem. A* **1997**, *101*, 1767 and references within.

(23) Papayannis, D. K.; Kosmas, A. M.; Melissas, V. S. *J. Phys. Chem. A* **2001**, *105*, 2209.

(24) Lee, T. J.; Dateo, C. E.; Rice, J. E. *Mol. Phys.* **1999**, *96*, 633.

(25) Papayannis, D. K.; Melissas, V. S.; Kosmas, A. M. *Phys. Chem. Chem. Phys.* **2003**, *5*, 2976.

(26) Drougas, E.; Kosmas, A. M. *Int. J. Quantum Chem.*, in press.